FFICE OF NAVAL RESEARCH

Grant N00014-90-J-1971

R&T Code 4131pc1

Technical Report No. 11

High Resolution Infrared Spectroscopy of Cyclobutane: A study of vibrational mode coupling involving large amplitude, low frequency modes

by

H. Li, C. Cameron Miller, and Laura A. Philips

Cornell University
Department of Chemistry
Ithaca, NY 14853-1301

Prepared for Publication
in the
Journal of Chemical Physics

October 26, 1993

HIGH RESOLUTION INFRARED SPECTROSCOPY OF CYCLOBUTANE: A STUDY OF VIBRATIONAL MODE COUPLING INVOLVING LARGE AMPLITUDE, LOW FREQUENCY MODES

H. Li, C. Cameron Miller, and Laura A. Philips, Department of Chemistry, Cornell University, Ithaca, New York, 14853-1301

Abstract

The high resolution IR spectrum of cyclobutane in a supersonic molecular beam was obtained for the region of 2981 to 2991 cm^{-1}. The spectrum reveals four overlapping bands suggestive of vibrational mode coupling in the C-H stretching region. Ground state combination differences demonstrate that these bands originate from 2 different ground states, the symmetric and asymmetric ring puckering states. Evidence of vibrational mode coupling is present in all four bands. The coupling depends on both J and the symmetry of the puckering state. A model coupling scheme involving two qualitatively different types of couplings is developed to explain the observed spectrum. Symmetry restrictions and the Interaction between molecular rotation and ring puckering qualitatively accounts for the dramatically different coupling behavior between the two ring puckering states.

I. Introduction

Previous work in the area of vibrational spectroscopy has suggested that the rate of intramolecular vibrational energy redistribution (IVR) can be linked to molecular size and structure.[1-20] More precisely, IVR rates are dictated by the specific details of the coupling between different vibrational modes. Studies using vibrational spectroscopy have suggested that some structural characteristics of a molecule can control the extent of vibrational mode coupling.[3-9,11-15,19] Many recent studies have focused on mid-sized organic molecules[1-29] which fall in the interesting regime between the low density of states limit, in which two well-defined individual states are coupled, and the statistical limit, in which a single state is randomly coupled to a bath of states.[1,21,24,27-29] In this intermediate regime, one can begin to

observe the correlation that occurs between vibrational mode coupling and molecular structure. Interesting mode coupling effects have been observed for systems that contain a low frequency, large amplitude mode. For example, unexpected couplings occur between high frequency hydrogen stretching modes and large amplitude, low frequency modes, such as torsions.[5,6,10,11,14,15] We seek to gain a better understanding of this coupling between disparate modes. Cyclobutane was chosen for this study of vibrational mode coupling because it is a mid-sized organic molecule with interesting structural characteristics and a large amplitude, low frequency mode.

The structure of cyclobutane has been of interest to chemists for decades.[30-36] As shown in Figure 1, two equilibrium geometries are possible for cyclobutane: 1) a structure of D_{4h} symmetry where all four carbon atoms are in the same plane; and 2) a structure of D_{2d} symmetry that has two equal energy puckered geometries with the planar geometry a local maximum in potential energy. The ring strain of cyclobutane favors the planar geometry to minimize the strain energy, while the repulsion between neighboring C-H bonds favors a puckered geometry in which the C-H bond is staggered rather than eclipsed. The equilibrium geometry will be a compromise between these two effects. Since the D_{4h} and D_{2d} groups have different IR and Raman selection rules, in principle one can determine the geometry using vibrational mode analysis and vibrational spectroscopy. Some early studies of cyclobutane attempted to perform such an analysis.[34,35] As a result of the overtones and perturbations in the spectrum, determining the equilibrium structure of cyclobutane by group symmetry alone, proved to be difficult.

The most definitive experiments on the equilibrium structure of cyclobutane, to date, confirmed that cyclobutane has a puckered structure with

a double-well potential surface.[30,32,33,37] The two minima correspond to two equivalent structures with a puckering angle of 29.5°. The height of the barrier between the two equivalent forms is only ~500cm^{-1}, which gives rise to tunneling splitting. In fact, the puckering tunneling splitting has been observed in the mid-IR region as hot bands.[32,33,35,37] Since cyclobutane does not have a permanent dipole moment, and the puckering mode is not an IR active mode, direct probing of the puckering mode is not possible. The most detailed information available about the puckering mode of cyclobutane was obtained through combination bands of IR-active modes in both the mid-IR region and the pure rotational spectrum of selectively deuterated species.[30] In particular, IR studies have demonstrated that the second lowest vibrational mode, the CH_2 rocking mode, couples extensively with the puckering mode.[32,33] The rocking angle of the CH_2 group is linearly correlated to the puckering angle, θ.[30,32,33] Microwave spectroscopy of the deuterated species resulted in a set of accurate rotational constants for deuterated cyclobutane, in both the ground and excited puckering states.[30] The calculated tunneling splitting was found to be 0.01 cm^{-1}. Combining both the IR and microwave results, leads to the puckering potential shown in Figure 2. The puckering potential, as expected, is highly anharmonic and best described by a 6th order polynomial expansion of the puckering coordinate. Note that due to the coupling of the CH_2 rocking motion with the puckering of cyclobutane, as shown in Figure 3, the effective reduced mass varies dramatically with the puckering coordinate.

The puckering coordinate of cyclobutane can be compared to other large amplitude, low frequency modes, such as torsional modes. Recently, in our laboratory[5-7,14,15] as well as others[4,9-13,15,38], many organic molecules containing torsions have been studied using high resolution IR spectroscopy.

The observed trends suggest a correlation between the conformational structure of molecules and vibrational mode coupling. The observed trend in a series of substituted ethanes[14,15], suggests that the strength of intramolecular interactions correlates with the extent of vibrational mode coupling. Cyclobutane, in a sense, offers an extreme case of intramolecular interaction, in which the C-C torsion is restricted by an additional C-C covalent bond. The trend in our study of substituted ethanes suggests that by increasing the intramolecular interaction in this manner, one would see more extensive mode coupling. In addition, cyclobutane is the first in a series of molecules we plan to study to explore the effects of ring-strain on mode coupling.

II. Experiment

The cyclobutane spectra reported in this paper were collected using an optothermal molecular beam spectrometer. The experimental apparatus has been described in detail elsewhere.[5] Briefly, the molecular beam was created by expanding a mixture of cyclobutane and helium through a 50 μm nozzle. The resulting free jet was skimmed with a 500 μm skimmer located 2.5 cm from the nozzle. The liquid helium cooled bolometer (Infrared Laboratories Inc.) was placed 20 cm from the nozzle in the flight path of the molecular beam. The molecular beam was crossed with the infrared laser, in a multipassing configuration, 2 cm from the nozzle.

An F-center laser (Burleigh FCL-20) was used to produce high resolution infrared radiation. The F-center laser was pumped by an Argon ion (Coherent, Innova 15) pumped dye laser (Coherent 599). The system produced 10 mW of tunable infrared radiation in the region of the C-H stretch of cyclobutane. To scan the F-center laser continuously, while remaining

single-mode, a Macintosh II computer was used to control both the laser end mirror and the intracavity etalon synchronously. To monitor the high resolution scanning of the laser, two external confocal etalons were used, a scanning 7.5 GHz etalon and a fixed 750 MHz etalon. The scanning etalon was used, with a Wavelength Monitor (Digital Specialties) to produce a sawtooth wave with a period equal to the free spectral range of the etalon. The sawtooth voltage signal from the wavelength monitor was used to detect and correct for discontinuities during the scans. The fixed etalon provided marker peaks 750 MHz apart which were later used to linearize the spectra. The etalon was calibrated daily with acetylene transitions of known frequency. The spectra were normalized for laser power fluctuations and bolometer desensitization. The final signal to noise ratio for the spectra was on the order of 130 to 1.

Cyclobutane was seeded into the molecular beam by passing the helium carrier gas through a stainless steel reservoir, containing the sample, prior to expansion. The reservoir was maintained at -55°C using a cryocool (NesLab) cooling bath. Variations in the bath temperature and the backing pressure of the carrier gas were used to control the rotational temperature of the sample. We obtained three spectra of cyclobutane at three different rotational temperatures ranging from 3 K to 10 K using backing pressures from 30 to 60 psig (2-4 atm).

Cyclobutane was synthesized via the Wurtz reaction. The method is described in detail elsewhere.[31,39] Briefly, lithium amalgam was used to reduce the alkyl halide through a ring closure to give the product. The reaction is the following:

$$BrCH_2CH_2CH_2CH_2Br \xrightarrow{Li/Hg} \overline{CH_2CH_2CH_2CH_2}$$

Lithium amalgam was prepared using the method of Alexander.[40] The freshly prepared lithium amalgam was refluxed with 1,4-dioxane, while 1,4-dibromobutane was added dropwise. The reflux was continued for up to 8 hours. The product was collected using a condensing tube with a dry-ice acetone cold trap at -55°C. The crude product was purified by distillation at room temperature. The product cyclobutane had a boiling point at 10°C and was further verified by an FTIR spectrum.

III. Results

A high resolution infrared spectrum of cyclobutane was collected with the molecular beam spectrometer described above. The spectrum was collected in the 2981-2991 cm^{-1} region, which corresponds to the excitation of the A_{2u} asymmetric C-H stretching vibration, the only IR active C-H stretch in this region which produces a C-type transition. Assigning quantum numbers to the individual transitions was performed by calculating spectra and comparing them to the experimental spectrum. As an initial guess the rotational constants were determined from the ground state geometry of the molecule based on previous work.[30,32] These ground state rotational constants were used for both the excited state and the ground state when calculating spectra. Similarities between the calculated and experimental spectrum were then used to assign peaks in the experimental spectrum and to refine the rotational constants. To confirm the quantum number assignment, the ground state rotational constants were determined by calculating combination differences on the experimental spectrum. Peak intensity variations as a function of temperature were used as a further check of quantum number assignments. Figure 4 shows stick spectra of cyclobutane measured at two different rotational temperatures.

Visual inspection, after partial assignment of the spectrum, clearly suggested that more than one rotational envelope are present in the spectrum. The general features of the rotationally resolved peaks suggest the presence of four vibrational bands. Two of the bands are significantly more intense than the others. All four transitions contain rotational structure that resemble a symmetric rotor. We labeled the two more intense bands as A and B, and the two less intense bands as C and D. The relative center frequencies of the four transitions are given in Table 1. An expanded section of the spectrum is shown in Figure 5, where peaks from the four different bands have been labeled.

Although transitions A and B have similar intensities, upon closer inspection, subtle differences between them are evident. Both bands exhibit peak fractionation, and when all the assigned transitions were fit to a simple rigid rotor model neither band A nor B fit within experimental uncertainty. When low J transitions in both bands A and B were fit using a rigid rotor Hamiltonian, both bands fit within experimental uncertainties. Combination differences revealed that peak fractionation results from perturbations in the excited vibrational state. Some examples of combination differences pairs are shown in Figure 6.

To fit transition A and B, the centroid of each fractionated peak was determined using the method of Lawrence and Knight.[41] The K structure is not well separated with our resolution in these two bands. The lack of K splitting added difficulty in assigning the fractionated peaks. Assignments were verified using intensity variations as a function of rotational temperature and by combination differences. The ground state rotational constants of band A were distinct from the ground state rotational constants of band B. The rotational constants for all of the bands are given in Table 1.

The difference in the ground state rotational constants for bands A and B, are consistent with the assignment of these two bands to the two lowest puckering states of cyclobutane, based on previous determinations of the rotational constants of these two vibrational states.[37] Note that although the rotational constants of the two bands are distinct, they are extremely similar, as one would expect of two states that result from a tunneling splitting calculated to be $0.01 cm^{-1}$.

The fitting error for bands A and B are quite similar. In both bands A and B, over 70 peaks were assigned. Due to the peak fractionation in bands A and B, we fit the ground state rotational constants using combination differences. The fitting error for the ground state combination differences was well within the experimental uncertainties. The large error in fitting bands A and B is consistent with the conclusion that transitions A and B are perturbed. The upper state information in A and B is obtained by a deconvolution of the spectrum, reducing the clumps of peaks to single transitions. The error was two and half times larger than the experimental uncertainties, as expected, because of intensity uncertainties (10%) used in the deconvolution process.

After fitting the two larger bands, we proceeded to fit the two small bands, C and D. The smaller intensities of these two bands made accurate assignments more challenging, and resulted in fitting errors that are slightly larger than the experimental uncertainties. The errors are not surprising considering that in both C and D a rigid rotor Hamiltonian was used in the fitting procedure, which did not account for either local perturbations or fractionation in the spectrum. The rotational constants and relative center frequencies for bands C and D are also given in Table 1. All of the quantum number assignments for the four different bands are given in Table 2. All

peaks of intensity 10% of the largest peak were assigned. The stick spectrum and the final calculated fits to the data are shown in Figure 7.

IV. Discussion

A) Assignment of the Four Bands

Because of the large frequency separation between the symmetric C-H stretching vibration and all other fundamental vibrations we can be certain that the extra features in the spectrum are not due to the excitation of a different near degenerate fundamental vibration. Other combination bands would be predicted to have transitions in the spectral region of the C-H stretch, however, the intensities of these transitions are expected to be much smaller than those observed here.

As described above, one of the more intense bands originates from the lowest puckering state, 0^+, of the ground vibrational state. The second intense band originates from the first excited puckering state, 0^-. IR selection rules restrict the symmetry of the puckering state in the excited C-H vibrational state. The following selection rules apply for the parallel C-H stretching transition measured here:

$$+ \leftrightarrow + \text{ and } - \leftrightarrow -$$

Based on these selection rules, the two intense bands can be assigned to be $0^+ \rightarrow 0^+$ and $0^- \rightarrow 0^-$. Previous calculations[30,32,33], consistent with previous experiments[32], estimated the separation between 0^+ and 0^- in the ground state to be 0.01 cm^{-1}. The center frequencies of A and B are 2986.1032 cm^{-1} and 2986.1826 cm^{-1}, respectively, which results in a frequency separation of 0.0794 cm^{-1}. The energy level diagram for the tunneling splitting in the ground and excited C-H stretching coordinate is shown in Figure 8. Assuming that the symmetric 0^+ puckering state of the excited C-H state should be at a lower

energy than the antisymmetric 0^- puckering state, band A is $0^+ \rightarrow 0^+$ and B is $0^- \rightarrow 0^-$. In addition, microwave experiments on deuterated cyclobutane suggested that the 0^- state has slightly larger rotational constants than the 0^+ state—consistent with our assignment.[30] This assignment results in a tunneling splitting of 0.09 cm^{-1} in the excited C-H stretching state. If all other parameters are constant, this larger splitting suggests a smaller tunneling barrier in the excited state. Because of our minimal knowledge of the excited state potential surface, this observation is only qualitative and does not account for other perturbations that may be present in the excited vibrational state.

Assignment of bands C and D, requires some additional discussion. Two possible explanations for the presence of C and D are: 1) the excited C-H vibrational state is split into two bands by vibrational mode coupling, or 2) these two transitions are simply hot bands from the 1^+ and 1^- puckering states of the ground state. Egawa et al.[37] studied the far IR CH_2 rocking vibrational spectrum of cyclobutane with a resolution of 0.0014 cm^{-1}. In their room temperature spectra, they were able to assign hot bands due to the 1^+ and 1^- levels. From the analysis of the hot bands, they were able to determine rotational constants for these two states. Our fitting suggest that A and C, and B and D share the same ground state rotational constants, which are in good agreement with the 0^+ and 0^- rotational constants of the data of Egawa et al., and distinct from their 1^+ and 1^- rotational constants. In addition, the temperature dependence of bands C and D are consistent with these bands originating from the same states as A and B, respectively. Thus, we conclude that the bands C and D indicate the presence of vibrational mode coupling in the excited C-H stretching vibrational state, in both the 0^+ and the 0^- puckering states. The tunneling splitting between the excited states of bands C

and D is calculated to be 0.06 cm^{-1} based on a ground state separation of 0.01 cm^{-1}

B) Vibrational Mode Coupling

To summarize the experimental spectrum and our assignments, we propose the following mode coupling scheme in cyclobutane. There are two distinct coupling mechanisms in cyclobutane, shown diagramatically in Figure 9. First, the 0^+ and 0^- states of the excited C-H stretching are each coupled to a single dark state with a large coupling matrix element. This first coupling gives rise to four distinct bands in the C-H stretching region of the spectrum. The origin of this first mode coupling is likely to be anharmonic coupling. In addition, each of these four perturbed states, couple to a manifold of dark states, which gives rise to further fractionation of the individual ro-vibrational transitions in each of the four bands. The extent of such couplings to the bath of dark states varies in each of the four states. There is a striking difference in the coupling in bands A and B. Coupling in A occurs starting at J=2 transitions while coupling in B is less dramatic and occurs only at larger values of J.

We can estimate the coupling matrix elements for the two different couplings mechanisms from the spectrum. The coupling which connects each bright state to a single dark state has a coupling matrix element of 0.05-0.1 cm^{-1}. The coupling mechanism that couples each of the four states to the bath states has a coupling matrix element of 0.001-0.005 cm^{-1}. This order of magnitude difference in coupling matrix element makes the effects of the two different coupling processes easily distinguishable in the spectrum, even by visual inspection.

The first coupling, of magnitude 0.05-0.1 cm^{-1}, couples each bright state to a single dark state. The identity of the dark state can be surmised by examining the possible modes that are candidates for coupling in the energy region 2980-2990 cm^{-1}. Not all of the states in this region are able to couple to the bright state. Since the dark state couples to both of the tunneling states, the dark state must have a + and - component. Based on the separation in the excited states, the tunneling states must be 0^+ and 0^-. The excited state rotational constants for bands A and B are very similar, and the constants for C and D are very similar. These similarities between excited state rotational constants provide additional evidence that the excited states for bands A and B, and C and D, are two tunneling doublets. Further elimination of possible candidates for coupling to the bright state is achieved by employing symmetry restrictions, discussed in the next section. After elimination of all inappropriate states, only one state remains. The coupled dark state is identified to be the state with 1 quantum of ring stretch (ring breathing), 1 quantum of CH_2 wag+twist+ring stretch, and 1 quantum of CH_2 rock+twist, using the notation of Annamalai and Keiderling.[42] The dark state identified is consistent with previous studies that the CH_2 rock couples well to the puckering motion.

C) Symmetry Group of Cyclobutane

In an attempt to account for the striking difference in coupling in bands A and B, the symmetry restrictions based on the symmetry of the puckering state were examined. Since bands A and B terminate in two different puckering states, 0^+ and 0^-, respectively, they will couple to different bath states dictated by coupling selection rules. Differences in the symmetry of the

wavefunctions will lead to different restrictions on the available bath states, and therefore could account for the differences observed in the spectrum.

For a non-rigid molecule like cyclobutane, a simple point group is not sufficient to model the puckering states. Permutation inversion (P.I.) group theory is necessary to describe this low frequency large amplitude motion. The analysis follows the discussion of Bunker.[43] For the 4 carbon atoms and 8 hydrogen atoms in cyclobutane, the P.I. group S_4xS_8xE has symmetry operations well in excess of a million. By the deletion of all unfeasible operations in the P.I. group, one reduces the group to the molecular symmetry (MS) group. The MS group of cyclobutane is D_{4h} rather than its point symmetry group D_{2d}. By performing proper symmetry operations, we can determine the equivalent rotation for each operation in the MS group. Using the symmetry of rotation, the symmetry representation of each rotational state can be determined. The nuclear spin statistical weights were also determined. Nuclear spin statistics determined using the standard P.I. group approach predict a variation in statistical weights of 40:60:36:60 for K=4n:4n+1:4n+2:4n+3. Such variations are not detectable with our intensity uncertainties given the fractionation of peaks.

The normal modes of cyclobutane from D_{2d} group were transformed to the new D_{4h} MS group. The puckering mode has B_{1u} symmetry and the C-H stretching mode of interest has A_{2u} symmetry. The 0^+ state of the first excited C-H stretching then has A_{2u} symmetry and the 0^- state has B_{2g} symmetry. These symmetry assignments of the different excited states are used in the next section to determine the density of states available for coupling to the 0^+ and 0^- states.

D) Puckering States

To calculate the density of states for cyclobutane, we made the approximation that all vibrational modes, other than the puckering mode, are uncoupled anharmonic oscillators, with 2% anharmonicity. The fundamental frequencies are taken from Ref. 42. To calculate the puckering energy levels we used the puckering potential of the ground state determined by Egawa et al. Their puckering potential was expanded to q^6 power, where q is the puckering coordinate:

$$V=aq^2+bq^4+cq^6 \qquad \text{Eq. (1)}$$

The complete puckering Hamiltonian involves kinetic as well as these potential terms. Following Egawa et al. and using standard procedure, the final Hamiltonian is written as:

$$H=\frac{1}{2\mu(q)}P_q^2+V(q) \qquad \text{Eq. (2)}$$

where $\mu(q)$ is the effective reduced mass of puckering, defined to be:

$$\mu(q)=\sum_i m_i\left(\frac{dr_i}{dq}\right)^2 \qquad \text{Eq. (3)}$$

where r_i is the position of i-th atom in cyclobutane. To account for the coupling between CH_2 rocking and ring puckering, the local CH_2 group is allowed to deviate from C_{2v} symmetry by angle β, where β is related to the puckering angle θ by:

$$\beta=\delta\theta \qquad \text{Eq. (4)}$$

with δ was determined to be 0.22 by both IR and microwave work.[30,32,33] Both $1/\mu(q)$ and V(q) were then expanded to the q^6 term. See Figure 10 for a plot of $\mu(q)$ versus q. As many as 100 harmonic oscillator wave functions were used to diagonalize the Hamiltonian, and the eigenvalues were determined. Our calculation agreed well with Egawa's experiment and similar calculations[32] for all the states observed (Table 3). Using this approach, we calculated the

puckering state eigenvalues up to the C-H stretching frequency. These frequencies were used to determine the density of states in the C-H stretching region.

E) Density of States

The density of dark states was calculated to be 7.5 states/cm^{-1} in the C-H stretching region, neglecting symmetry considerations. If symmetry restrictions are included there are 1.5 states/cm^{-1} for A_{2u} symmetry and 1.0 state/cm^{-1} for B_{2g} symmetry in the 10 cm^{-1} window surrounding the C-H stretching frequency. In the experimental spectrum, the onset of peak fractionation occurs at J=2 for band A and J=4 for band B. Peaks in band A (J=2~5) are fractionated into four peaks, indicating coupling to three dark states. Band B (J=4~6) contains doublets, indicating coupling to one dark state. Band A, which exhibits mode coupling to 3 dark states has been assigned to the 0^+ transition and band B, which exhibits coupling to one dark state, has been assigned to the 0^- transition (see above). The calculation suggests that the 0^+ state with A_{2u} symmetry will couple to 50% more dark states than the 0^- state with B_{2g} symmetry. Thus, the experimental data are qualitatively consistent with the calculation. Quantitatively, the coupling in band A is suggestive of a larger density of coupled states than the calculation predicts.

Additional coupling could be introduced by the interaction of vibration and rotation. Inspection of the puckering Hamiltonian (Eq. 2) reveals that interaction between vibration and molecular rotation is present through a kinematic coupling term. The ring puckering will preserve the symmetric rotor character of cyclobutane, so K will remain a good quantum in this model. The fact that the reduced mass and rotational constants vary as a function of the puckering coordinate, however, allows kinematic coupling

between different puckering states, within restrictions due to symmetry. Note that this coupling would be present in both 0^+ and 0^- states. Allowing for this additional coupling, a very small J-dependence is predicted, and the overall magnitude of the coupling is almost unchanged. Thus, the different coupling behavior of 0^+ and 0^- states predicted by our model is in qualitative agreement with the trend observed experimentally, as shown in the diagram in Figure 11.

In addition to the work presented here, an attempt was made to measure the overtone spectrum of cyclobutane with the help of J. Timmermans in Prof. K. Lehmann and Prof. G. Scoles' group at Princeton University. The FTIR of cyclobutane in the overtone region indicates a relatively weak absorption in the 5918 cm^{-1} region. The absorption is sufficiently strong that the overtone should be observable with the Princeton apparatus. A total of 40 cm^{-1} was scanned in the vicinity of 5918 cm^{-1}, but no signal was detected. One possible explanation is the presence of extensive mode coupling in the overtone region which results in a large number of molecular eigenstates over which the oscillator strength is distributed. The density of states in the overtone region was calculated to be approximately 1300 states/cm^{-1}, most of which contain large numbers of quanta of ring puckering. The lack of observation of spectral features, however, limits our ability to draw conclusions concerning mode coupling in this spectral region.

V. Conclusions

Two qualitatively distinct types of mode couplings were observed in the asymmetric C-H stretching of cyclobutane. The symmetric and asymmetric puckering state is each coupled to a single dark state with a large coupling matrix element. The coupled dark state is identified to be the state

with 1 quantum of ring stretch (ring breathing), 1 quantum of CH_2 wag+twist+ring stretch, and 1 quantum of CH_2 rock+twist, using the notation of Annamalai and Keiderling.[42] Each of the four perturbed states are then further coupled to a bath of dark states with small coupling matrix elements, which lead to four overlapping, peak-fractionated bands in the 2986 cm^{-1} region. The coupling to the bath states shows J-dependence and most interestingly, dramatically different coupling behavior between the symmetric and asymmetric tunneling puckering states. The symmetric puckering state couples more extensively to the bath states than the almost degenerate asymmetric state.

To explain the experimental results, a model which takes into account the interaction between molecular rotation and ring puckering is used, along with P.I. group theory. The calculation is in qualitative agreement with the experimental data. This symmetry effect is suggested to play a role in the observed difference in coupling behavior among nearly degenerate states.

The comparison of these results to those of previous work on similar sized molecules with large amplitude, low frequency modes provides additional insight into the mode coupling behavior. In most previous work, the low frequency, large amplitude motion involved torsional motion.[5,6,10,11,14,15] In our previous work on substituted ethanes, we suggested that intramolecular interactions that effect torsional modes, can enhance mode coupling between states involving those torsional modes.[5,6,14,15] As noted above, one can view ring puckering in cyclobutane as an extremely hindered torsion, in which the barrier to internal rotation about any C-C bond is essentially infinite because of the covalently bonded ring structure. If intramolecular interactions enhance mode coupling, we would expect that cyclobutane would exhibit extensive mode coupling involving the

low frequency, large amplitude mode. The results presented here demonstrate that cyclobutane does exhibit such mode coupling involving the low frequency, large amplitude ring puckering mode. These results support our suggestion that intramolecular interactions enhance vibrational mode coupling involving low frequency, large amplitude modes.

Acknowledgments: The authors would like to thank: Joep Timmermans, Prof. Kevin K. Lehmann and Prof. G. Scoles for their collaboration on the overtone experiment; Prof. J. Burlitch for the loan of equipment used in the synthesis of cyclobutane; and Dr. Philip Bunker for helpful discussions on permutation inversion group theory. This work is supported by: The National Institute of Health under grant #08-R9N527039A, The Office of Naval Research under grant #N00014-90-J-1971, and The Petroleum Research Fund administered by The American Chemical Society.

(1) K. K. Lehmann, B. H. Pate and G. Scoles, J. Chem. Phys., **93**, 2152-2153 (1990).

(2) K. K. Lehmann, B. H. Pate and G. Scoles, Jerusalem Symposium on Quantum Chemistry and Biochemistry, **24**, 17-23 (1991).

(3) G. A. Bethardy and D. S. Perry, J. Mol. Spectrosc., **144**, 304-309 (1990).

(4) G. A. Bethardy and D. S. Perry, J. Chem. Phys., **98**, 6651-6664 (1993).

(5) C. L. Brummel, S. W. Mork and L. A. Philips, J. Chem. Phys., **95**, 7041-7053 (1991).

(6) C. L. Brummel, S. W. Mork and L. A. Philips, J. Am. Chem. Soc., **113**, 4342-4343 (1991).

(7) C. L. Brummel, M. Shen, K. B. Hewett and L. A. Philips, J. Opt. Soc. Am. B, in press (1993).

(8) A. M. de Souza, D. Kaur and D. S. Perry, J. Chem. Phys., **88**, 4569-4578 (1988).

(9) E. R. Kerstel, K. K. Lehmann, T. F. Mentel, B. H. Pate and G. Scoles, J. Phys. Chem., **95**, 8282-8293 (1991).

(10) J. Go, G. A. Bethardy and D. S. Perry, J. Phys. Chem., **94**, 6153-6156 (1990).

(11) J. E. Gambogi, R. P. L'Esperance, K. K. Lehmann, B. H. Pate and G. Scoles, J. Chem. Phys., **98**, 1116-1122 (1993).

(12) A. McIlroy and D. J. Nesbitt, J. Chem. Phys., **91**, 104-113 (1989).

(13) A. McIlroy and D. J. Nesbitt, J. Chem. Phys., **92**, 2229-2243 (1990).

(14) C. C. Miller, M. Shen and L. A. Philips, J. Phys. Chem., **97**, 537-539 (1993).

(15) S. W. Mork, C. C. Miller and L. A. Philips, J. Chem. Phys., **97**, 2971-2981 (1992).

(16) C. S. Parmenter, J. Phys. Chem., **86**, 1735-1750 (1982).

(17) C. S. Parmenter, Faraday Discuss. Chem. Soc., **75**, 7-22 (1983).

(18) C. S. Parmenter and B. M. Stone, J. Chem. Phys., **84**, 4710-4711 (1986).

(19) B. H. Pate, K. K. Lehmann and G. Scoles, J. Chem. Phys., **95**, 3891-3916 (1991).

(20) A. Stuchebrukhov, S. Ionov and V. Letokhov, J. Phys. Chem., **93**, 5357-5365 (1989).

(21) P. M. Felker and A. H. Zewail, Chem. Phys. Lett., **102**, 113-119 (1983).

(22) C. C. Matens and W. P. Reinhardt, J. Chem. Phys., **93**, 5621-5633 (1990).

(23) D. B. McDonald and S. A. Rice, J. Chem. Phys., **74**, 4893-4906 (1981).

(24) D. B. McDonald, G. R. Fleming and S. A. Rice, Chem. Phys., **60**, 335-345 (1981).

(25) D. J. Nesbitt, Jerusalem Symposium on Quantum Chemistry and Biochemistry, **24**, 113-126 (1991).

(26) R. E. Smalley, J. Phys. Chem., **86**, 3504-3512 (1982).

(27) A. H. Zewail, Faraday Discuss. Chem. Soc., **75**, 315-330 (1983).

(28) J. S. Baskin, M. Dantus and A. H. Zewail, Chem. Phys. Lett., **130**, 473-481 (1986).

(29) R. D. Levine and J. Jortner, Jerusalem Symposium on Quantum Chemistry and Biochemistry, **24**, 535-571 (1991).

(30) W. Caminati, B. Vogelsanger, R. Meyer, G. Grassi and A. Bauder, J. Mol. Spectrosc., **131**, 172-184 (1988).

(31) J. S. Chickos, J. Org. Chem., **44**, 780-784 (1979).

(32) T. Egawa, T. Fukuyama, S. Yamamoto, F. Takabayashi, H. Kambara, T. Ueda and K. Kuchitsu, J. Chem. Phys., **86**, 6018-6026 (1987).

(33) T. Egawa, S. Yamamoto, T. Ueda and K. Kuchitsu, J. Mol. Spectrosc., **126**, 231-239 (1987).

(34) T. P. Wilson, J. Chem. Phys., **11**, 369-376 (1943).

(35) T. Ueda and T. Shimanouchi, J. Chem. Phys., **49**, 470-471 (1968).

(36) G. W. J. Rathjens, N. K. Freeman, W. D. Gwinn and K. S. Pitzer, J. Chem. Phys., **75**, 5634-5642 (1953).

(37) T. Egawa, S. Yamamoto and K. Kozo, J. Mol. Spectrosc., **129**, 72-85 (1988).

(38) D. Moss, C. S. Parmenter and G. E. Ewing, J. Chem. Phys., **86**, 51-61 (1986).

(39) D. S. Conor and E. R. Wilson, Tetrahedron Lett., 4925-4929 (1967).

(40) J. Alexander and G. S. K. Rao, J. Chem. Ed., **47**, 277 (1970).

(41) W. D. Lawrence and A. E. W. Knight, J. Phys. Chem., **89**, 917-925 (1985).

(42) A. Annamalai and T. A. Keiderling, J. Mol. Spectrosc., **109**, 46 (1972).

(43) P. R. Bunker Molecular Symmetry and Spectroscopy; Academic Press, Inc.: 1979.

Figure Captions

Figure 1. The figure shows the two possible geometries of cyclobutane: (a) puckered with D_{2d} symmetry; and (b) planar with D_{4h} symmetry.

Figure 2. The schematic diagram above depicts the puckering potential of cyclobutane derived from IR and microwave results. The puckering barrier is 510 cm^{-1} and the puckering angle for the equivalent geometries is 29.5 degrees.

Figure 3. The diagram shows how the puckering coordinate q, the puckering angle θ and the coupling factor, $\beta=\delta\theta$, between CH_2 rocking and ring puckering δ are defined.

Figure 4. The experimental spectrum above shows the C-H stretching region of cyclobutane measured at two different rotational temperatures.

Figure 5. The above section of the experimental spectrum shows the four overlapping bands with varying degree of perturbations. There are two intense bands, A and B, and two weak bands, C and D.

Figure 6. Each panel in the figure shows two sets of transitions to the same excited state. The left panel shows two transitions to the 3_2 excited state which originate from two different ground states. The right panel shows two transitions to the 4_2 excited state. The similarity of the patterns in frequency and intensities of the peaks demonstrate the presence of vibrational mode coupling. The peaks labeled with (*) are features due to other transitions.

Figure 7. The two spectra above represent comparison of a calculated spectrum and the experimental results. The calculated spectrum consists of four bands.

Figure 8. The energy level diagram depicts the tunneling splitting in the ground and excited C-H stretching state.

Figure 9. The proposed mode coupling scheme in cyclobutane shown diagramatically, contains two different coupling mechanisms. First, the 0^+ and 0^- of the excited C-H stretching state are coupled to a single dark state with a large coupling matrix element. Second, the four strongly perturbed states couple to a bath of dark states with a smaller coupling matrix element.

Figure 10. The plot represents the effective reduced mass of ring puckering as a function of puckering coordinate q including the interaction between ring puckering and CH_2 rocking.

Figure 11. The diagram represents the coupling of the four different bands to the bath states as determined by the symmetries of the states.

Table Captions

Table 1. Presented in the table are rotational constants A and B, the difference in the C rotational constant, ΔC, and the center frequencies of the four bands observed experimentally. Notice that ΔC for bands C and D is much larger than for bands A and B. The large ΔC values for bands C and D allow us to resolve the K structure. This large change in C is consistent with our conclusion that the perturbing dark state contains CH_2 rocking.

Table 2. Shown below are the calculated and experimental frequencies for the assigned transitions in the spectrum of C-H stretching of cyclobutane. The transitions are labeled by their ground and excited state J and K_C quantum numbers. The relative experimental intensities are also given. In bands A and B, presented in part (a) and (b), respectively, each calculated frequency may have more than one quantum number assignment due to the unresolved K structure. These bands also exhibit peak fractionation which is presented in the table as multiple experimental frequencies for a single calculated frequency. In bands C and D, presented in parts (c) and (d), respectively, the K structure is resolved and the weak intensities of these bands prevent us from identifying peak fractionation.

Table 3. Calculated ring puckering transition frequencies in the ground state compared to experimental frequencies.

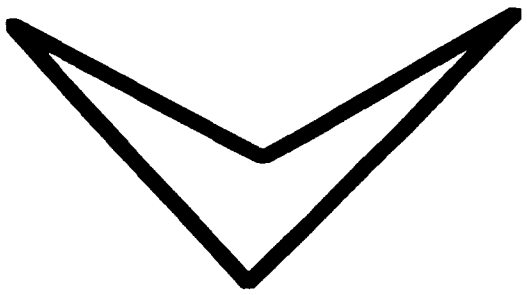

D_{2d}

(a)

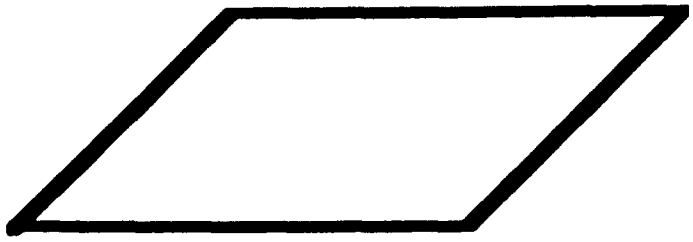

D_{4h}

(b)

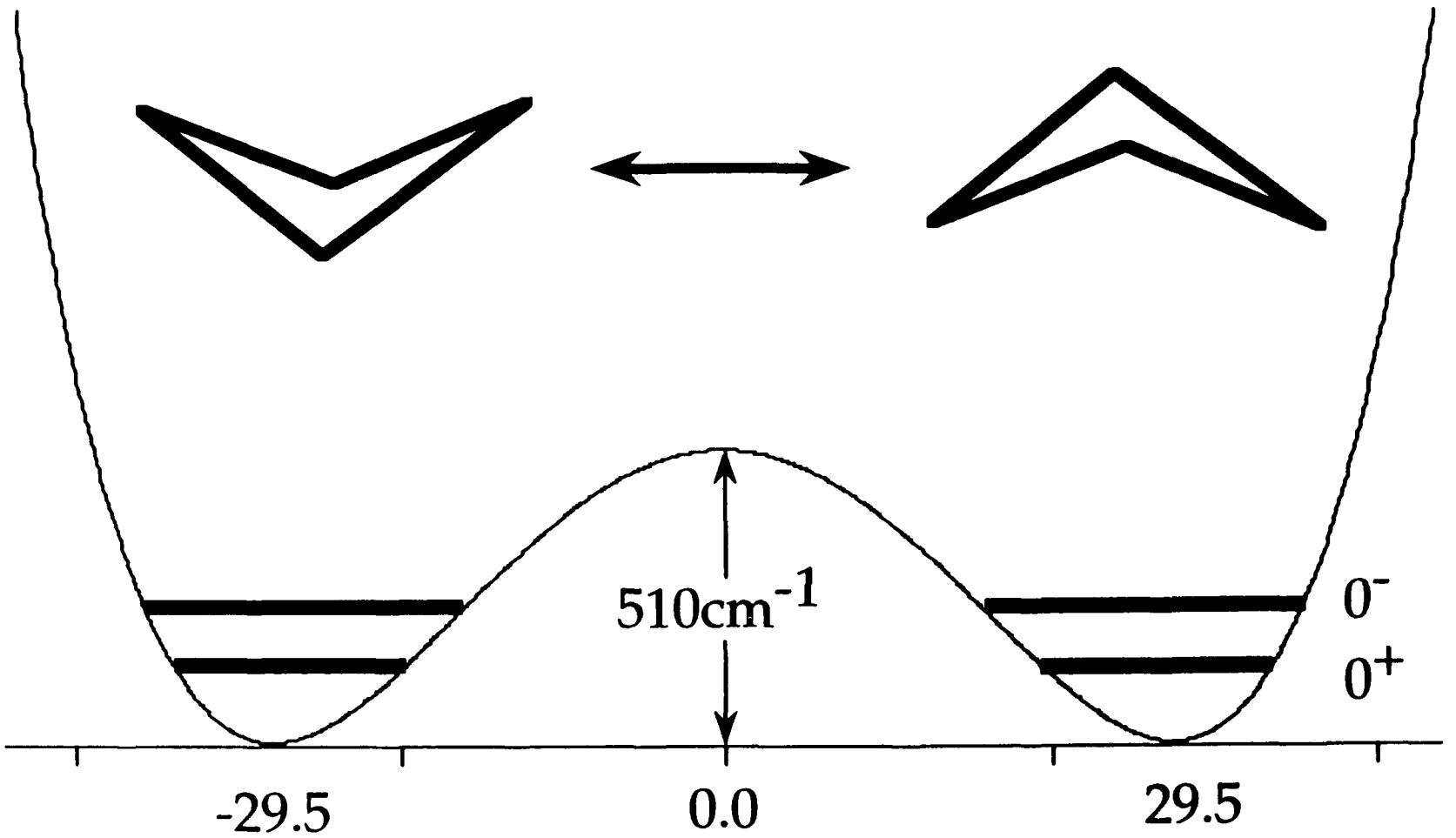
510cm-1
0-
0+
-29.5
0.0
29.5
Puckering Angle

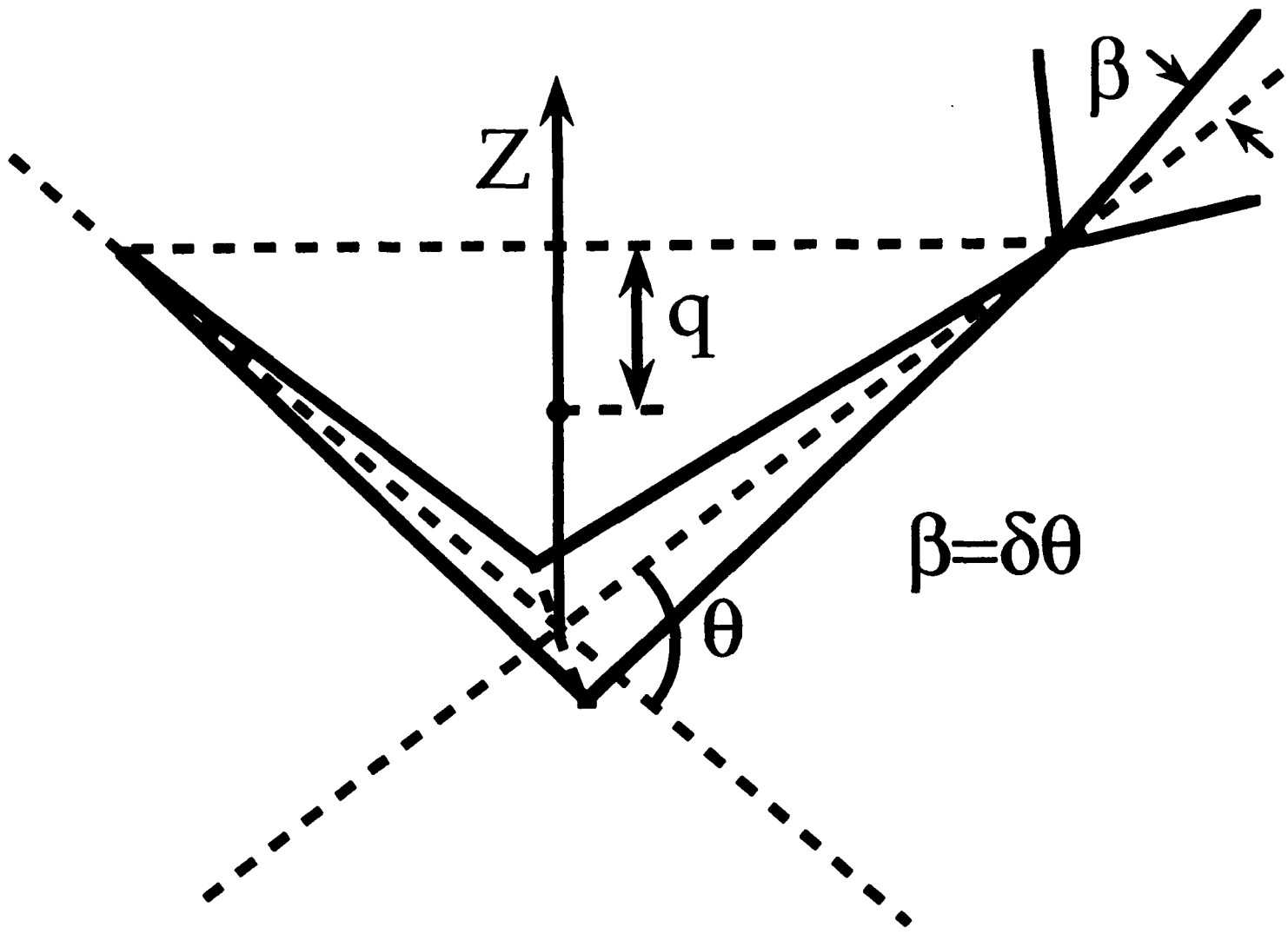
z
q
β
θ
β=δθ

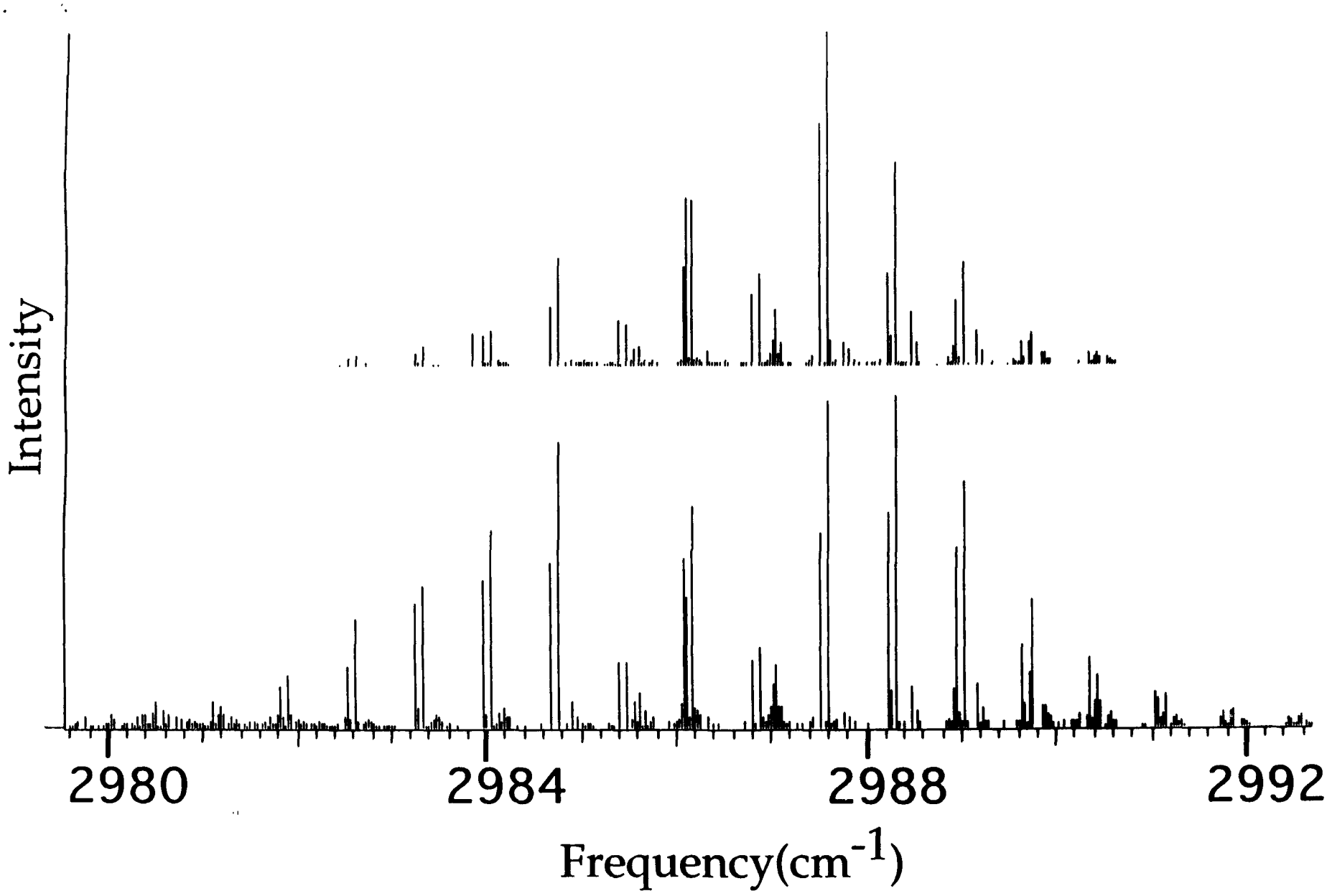
Intensity
2980
2984
2988
2992
Frequency(cm-1)

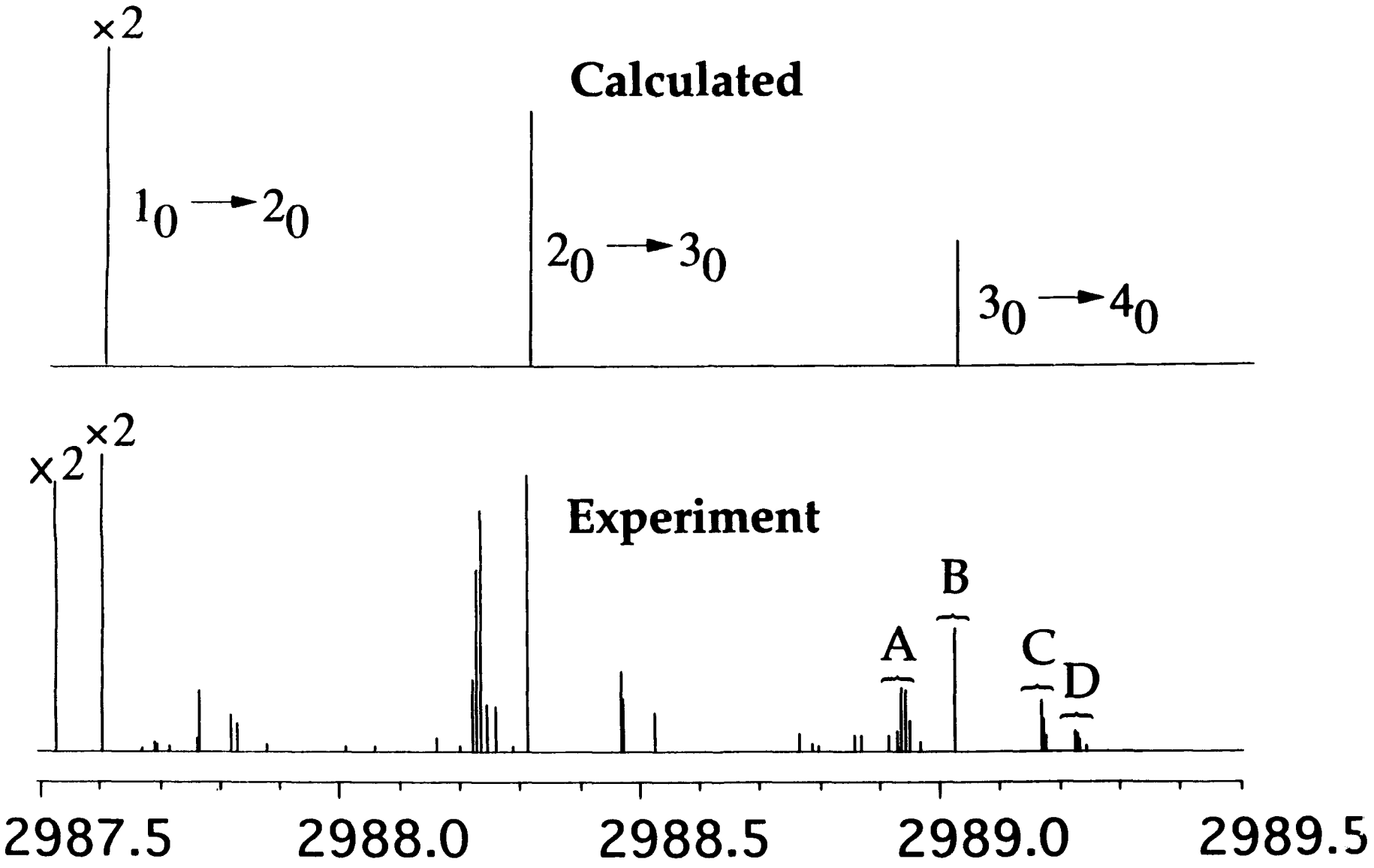
×2
Calculated
$1_0 \rightarrow 2_0$
$2_0 \rightarrow 3_0$
$3_0 \rightarrow 4_0$
×2
×2
Experiment
A
B
C
D
2987.5
2988.0
2988.5
2989.0
2989.5

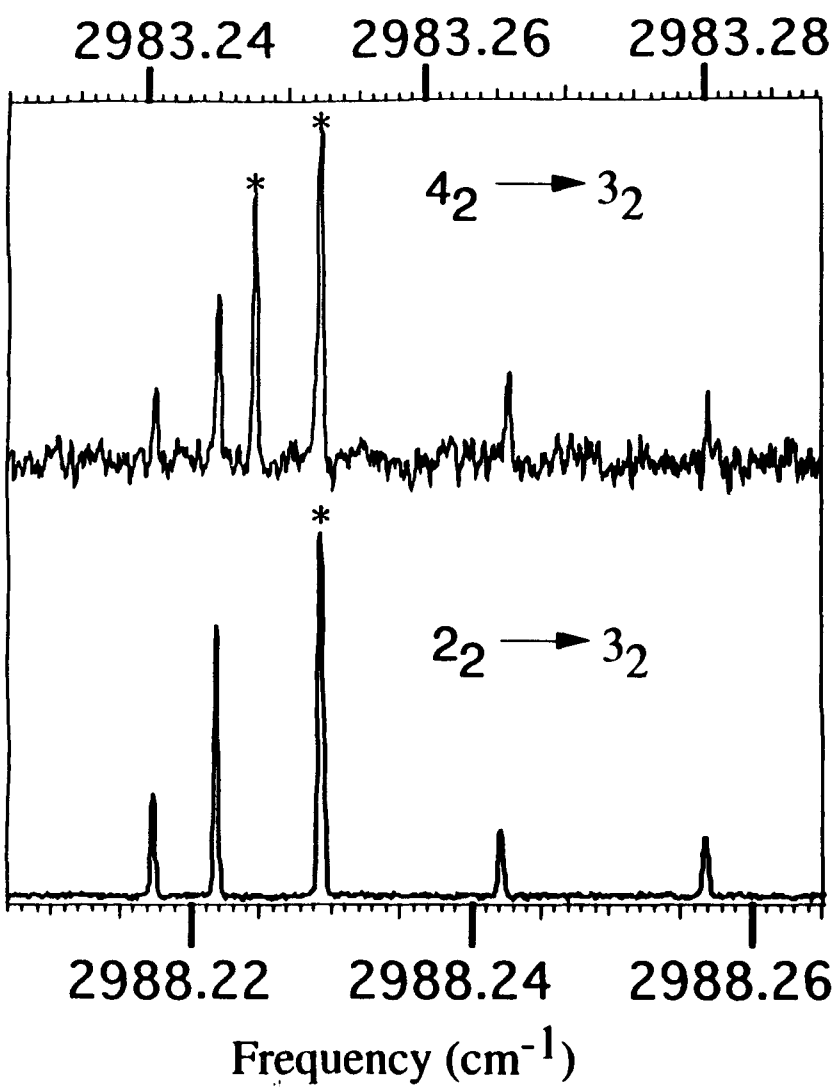
2983.24
2983.26
2983.28
$4_2 \rightarrow 3_2$
$2_2 \rightarrow 3_2$
2988.22
2988.24
2988.26
Frequency (cm^{-1})

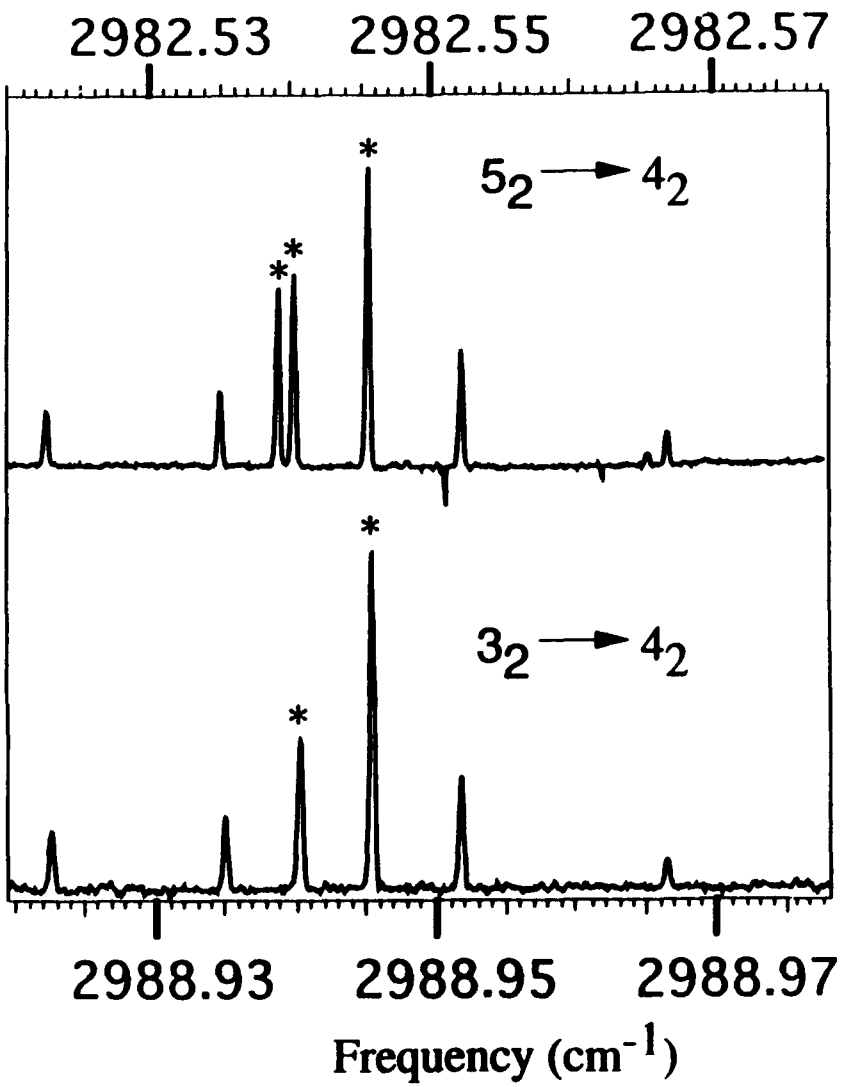
2982.53
2982.55
2982.57
$5_2 \rightarrow 4_2$
$3_2 \rightarrow 4_2$
2988.93
2988.95
2988.97
Frequency (cm^{-1})

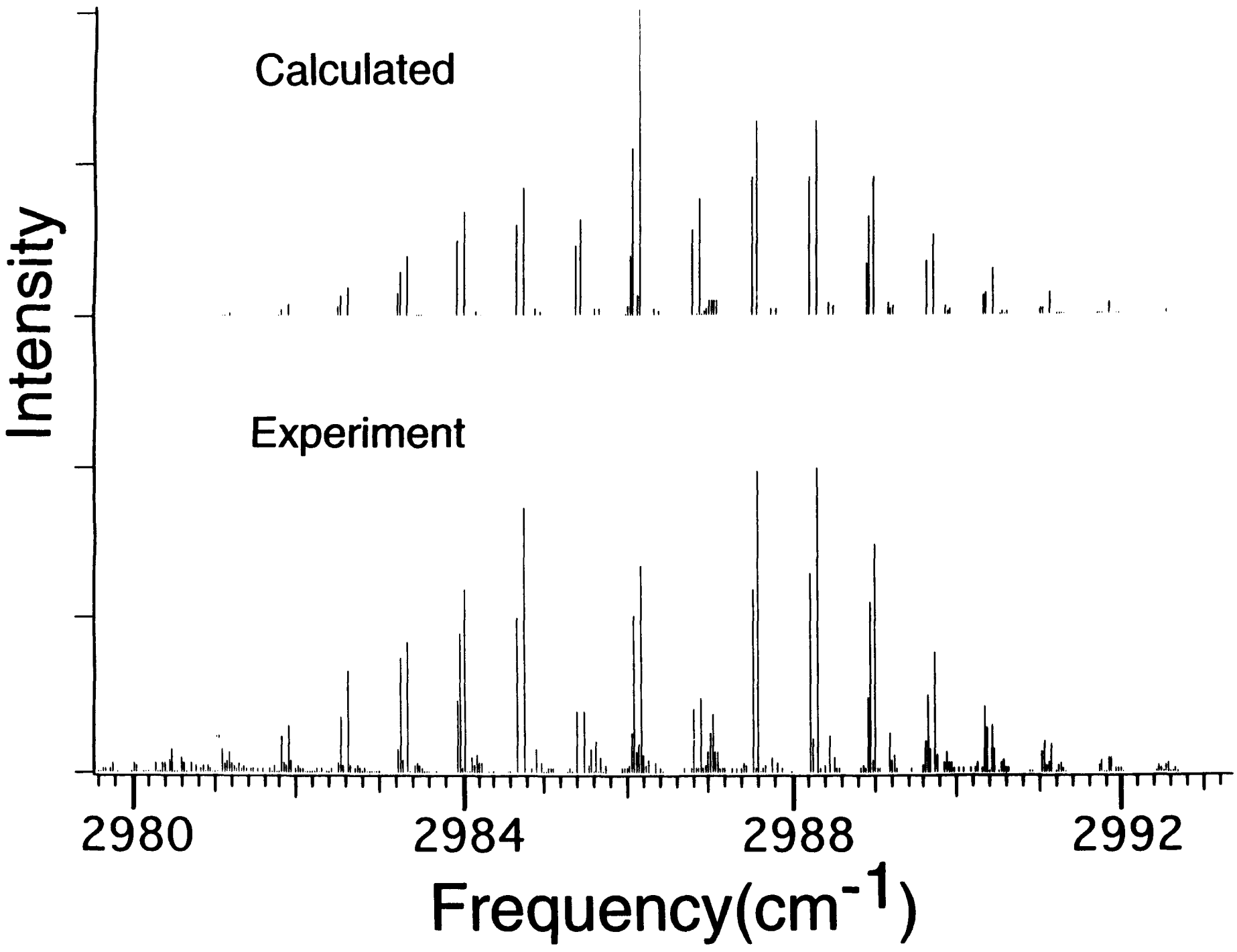
Calculated
Experiment
Intensity
2980
2984
2988
2992
Frequency(cm-1)

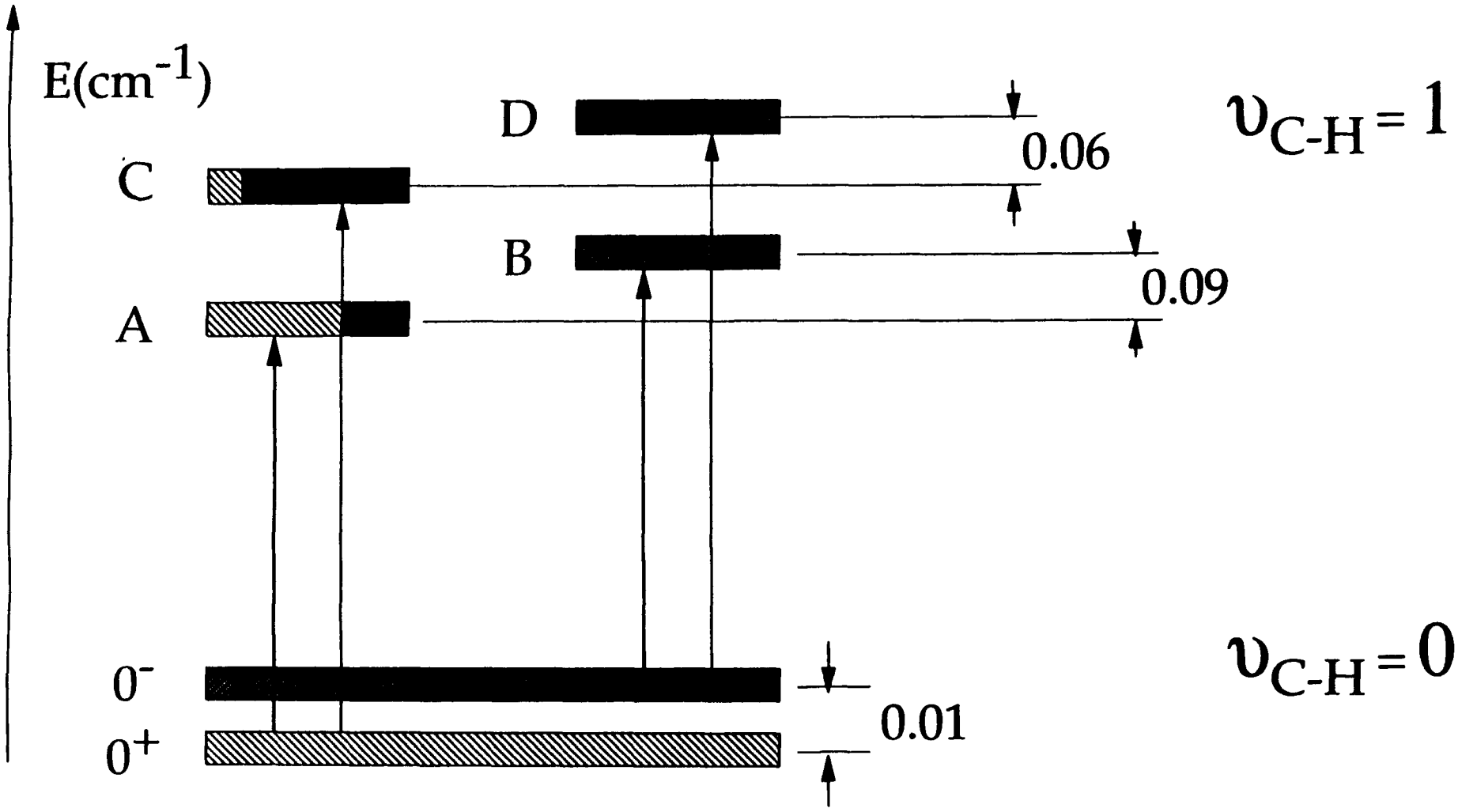
E(cm-1)
D
C
B
A
0.06
0.09
υC-H = 1
υC-H = 0
0-
0+
0.01

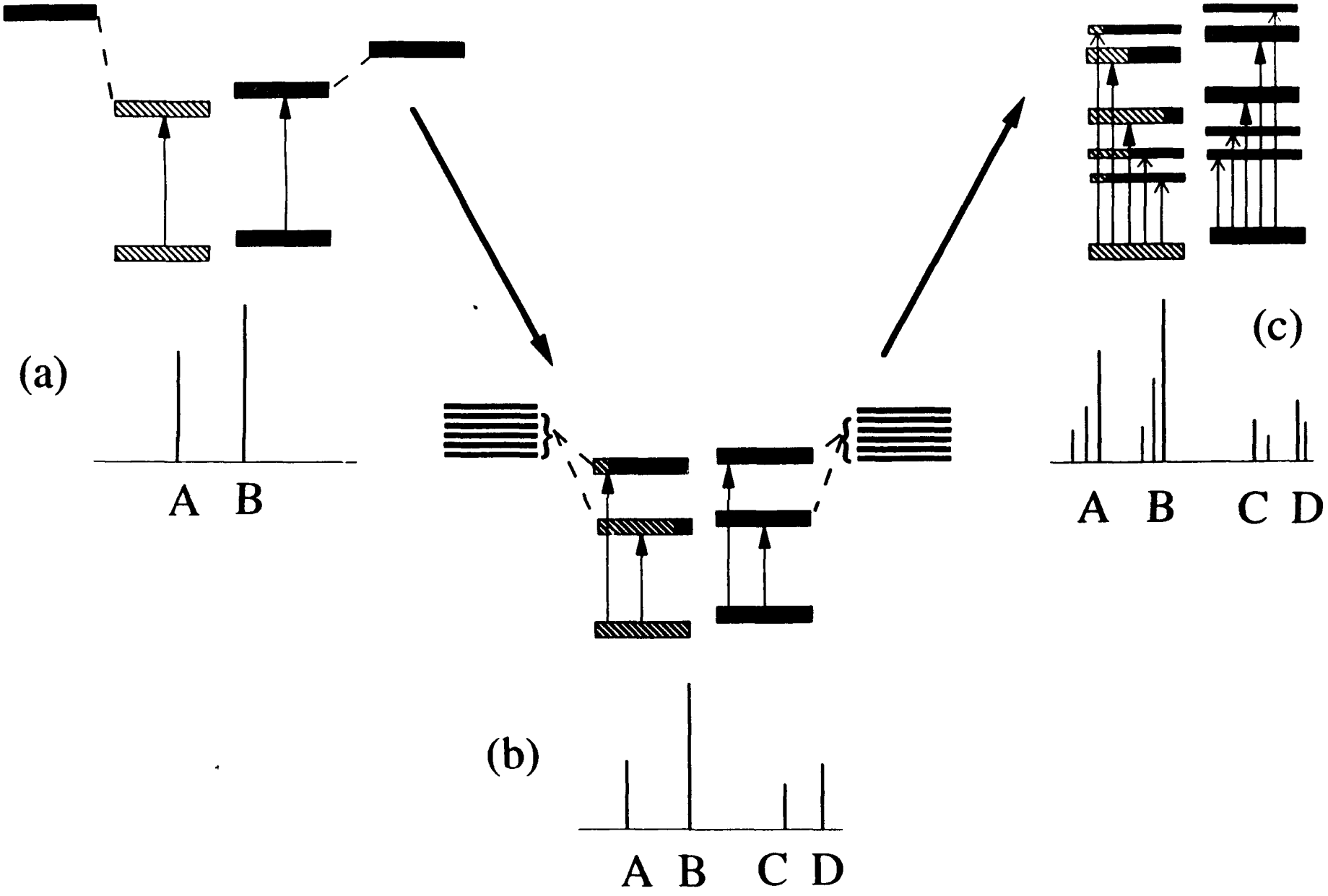
(a)
A B
(b)
A B C D
(c)
A B C D

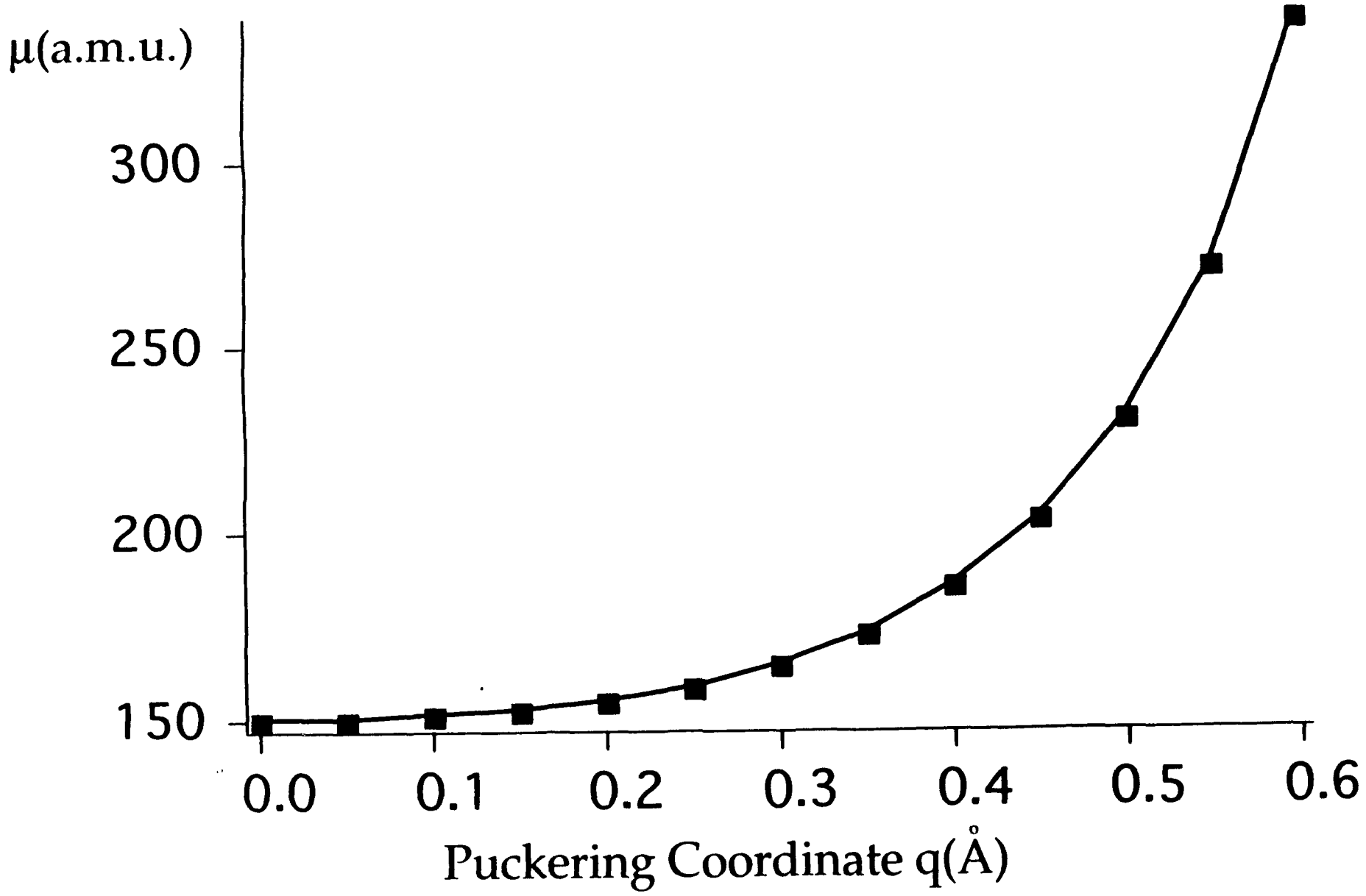
μ(a.m.u.)
300
250
200
150
0.0
0.1
0.2
0.3
0.4
0.5
0.6
Puckering Coordinate q(Å)

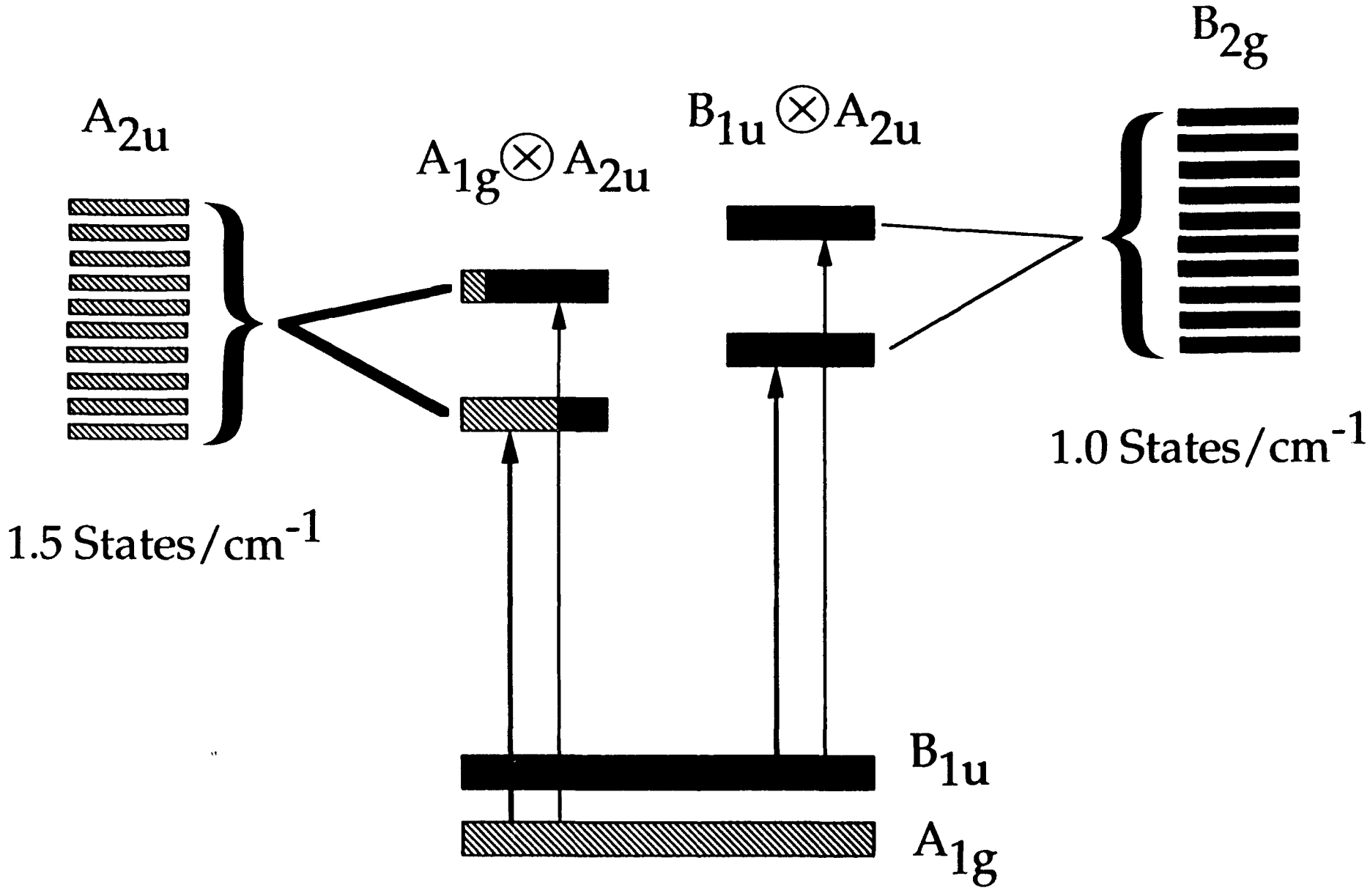
B_{2g}
A_{2u}
$B_{1u} \otimes A_{2u}$
$A_{1g} \otimes A_{2u}$
1.0 States/cm^{-1}
1.5 States/cm^{-1}
B_{1u}
A_{1g}

Bands	A"(cm^{-1})	B"(cm^{-1})	A'(cm^{-1})	B'(cm^{-1})	$\Delta C(cm^{-1})$	υ_0 (cm^{-1})
	Ground State		Excited State		C"-C'	
A	0.35581(3)	0.35581(3)	0.3553(1)	0.3553(1)	0.0010	2986.1032(3)
B	0.35583(3)	0.35575(3)	0.3556(1)	0.3551(1)	0.0004	2986.1826(6)
C	0.35581(3)	0.35581(3)	0.35444(5)	0.35444(4)	0.0026	2987.0568(4)
D	0.35578(5)	0.35578(3)	0.35457(3)	0.35454(3)	0.0031	2987.1112(6)

Table 2

(a) Assignment of Band A

Standard Dev = 0.0010 cm^{-1}

J' K_c'	J'' K_c''	Calc. ν	Experimental ν	I
0_0	1_0	2985.393	2985.3913	.20
1_1	2_1	2984.680	2984.6794	.56
1_0	2_0			
1_1	1_1	2986.103	2986.1023	.40
1_0	0_0	2986.815	2986.8143	0.20
2_2	3_2	2983.965	2983.9622	0.23
			2983.9629	0.15
			2983.9870	0.41
			2983.9959	0.01
2_1	3_1	2983.967	2983.9666	0.45
2_0	3_0			
2_2	2_2	2986.100	2986.0961	0.34
			2986.0969	0.24
			2986.1213	0.07
			2986.1302	0.03
2_1	2_1	2986.101	2986.1001	0.18
2_1	1_1	2987.525	2987.5246	0.59
2_0	1_0			
3_3	4_3	2983.248	2983.2472	0.25
3_2	4_2	2983.251	2983.2389	0.08
			2983.2442	0.19
			2983.2645	0.06
			2983.2792	0.05
3_1	4_1	2983.253	2983.2523	0.37
3_0	4_0			
3_3	3_3	2986.094	2986.0938	0.51
3_2	3_2	2986.097	2986.0856	0.06
			2986.0909	0.13
			2986.1121	0.05
			2986.1262	0.02
3_1	3_1	2986.099	2986.0990	0.05
3_2	2_2	2988.232	2988.2218	0.19
			2988.2266	0.36
			2988.2466	0.11
			2988.2614	0.07
3_1	2_1	2988.233	2988.2343	0.65
3_0	2_0			
4_4	5_4	2982.529	2982.5305	0.11
4_3	5_3	2982.533	2982.5319	0.13
4_2	5_2	2982.536	2982.5112	0.03
			2982.5256	0.05
			2982.5465	0.09
			2982.5641	0.03
4_1	5_1	2982.538	2982.5382	0.18
4_0	5_0			
4_4	4_4	2986.087	2986.0878	0.33
4_3	3_3	2988.937	2988.9361	0.24
4_2	3_2	2988.940	2988.9150	0.09
			2988.9298	0.12
			2988.9499	0.18
			2988.9674	0.05
4_1	3_1	2988.942	2988.9423	0.55
4_0	3_0			
5_5	6_5	2981.808	2981.7896	0.01
			2981.8006	0.01
			2981.8109	0.07
5_4	6_4	2981.813	2981.8128	0.09
5_3	6_3	2981.817	2981.8137	0.08
5_2	6_2	2981.820	2981.7727	0.01
			2981.8024	0.04
			2981.8269	0.04
			2981.8452	0.03
5_1	6_1	2981.821	2981.8219	0.12
5_0	6_0			
5_5	5_5	2986.077	2986.0593	0.01
			2986.0694	0.02
			2986.0800	0.18
5_4	4_4	2989.640	2989.6409	0.13
5_3	4_3	2989.644	2989.6417	0.18
5_2	4_2	2989.647	2989.6003	0.02
			2989.6306	0.10
			2989.6544	0.07
			2989.6730	0.07
5_1	4_1	2989.649	2989.6496	0.25
5_0	4_0			

(b) Assignment of Band B

Standard Dev = 0.0010 cm^{-1}

J' K_c'	J" K_c"	Calc. ν	Experimental ν	I
0_0	1_0	2985.471	2985.4705	0.20
1_1	2_1	2984.759	2984.7577	0.86
1_0	2_0			
1_1	1_1	2986.182	2986.1813	0.51
1_0	0_0	2986.894	2986.8925	0.24
2_2	3_2	2984.046	2984.0455	0.39
2_1	3_1			
2_0	3_0	2984.046	2984.0463	0.60
2_1	2_1	2986.181	2986.1806	0.25
2_2	2_2	2986.180	2986.1799	0.68
2_1	1_1	2987.604	2987.6042	0.99
2_0	1_0			
3_3	4_3	2983.332	2983.3322	0.25
3_2	4_2	2983.333	2983.3326	0.30
3_1	4_1			
3_0	4_0	2983.333	2983.3334	0.33
3_3	3_3	2986.178	2986.1783	0.53
3_2	3_2	2986.179	2986.1787	0.25
3_1	3_1			
3_2	2_2	2988.314	2988.3134	0.59
3_1	2_1	2988.314	2988.3142	1.00
3_0	2_0			
4_4	5_4	2982.617	2982.6145	0.15
			2982.6553	0.02
4_3	5_3	2982.619	2982.6196	0.33
4_2	5_2			
4_1	5_1	2982.620	2982.6205	0.22
4_0	5_0			
4_4	4_4	2986.175	2986.1719	0.41
			2986.2132	0.05
4_3	4_3	2986.177	2986.1771	0.23
4_2	4_2			
4_3	3_3	2989.023	2989.0231	0.75
4_2	3_2			
4_1	3_1	2989.024	2989.0240	0.50
4_0	3_0			
5_5	6_5	2981.902	2981.8998	0.07
			2981.9212	0.01
5_4	6_4	2981.903	2981.8930	0.08
			2981.9299	0.04
5_3	6_3	2981.905	2981.9047	0.16
5_2	6_2			
5_1	6_1	2981.906	2981.9054	0.14
5_0	6_0			
5_5	5_5	2986.171	2986.1667	0.13
			2986.1890	0.02
5_4	5_4	2986.173	2986.1636	0.10
			2986.2001	0.06
5_3	5_3	2986.175	2986.1752	0.09
5_2	5_2			
5_4	4_4	2989.731	2989.7208	0.16
			2989.7576	0.06
5_3	4_3	2989.733	2989.7321	0.39
5_2	4_2			
5_1	4_1	2989.733	2989.7328	0.32
5_0	4_0			
6_6	7_6	2981.186	2981.1836	0.04
			2981.1945	0.01
6_5	7_5	2981.187	2981.1656	0.03
			2981.1827	0.05
			2981.2056	0.04
6_4	7_4	2981.190	2981.1897	0.06
6_3	7_3			
6_2	7_2	2981.191	2981.1904	0.07
6_1	7_1			
6_0	7_0			
6_6	6_6	2986.167	2986.1620	0.09
			2986.1729	0.02
6_5	5_5	2990.434	2990.4177	0.08
			2990.4342	0.11
			2990.4577	0.08
6_4	5_4	2990.440	2990.4409	0.15
6_3	5_3			
6_2	5_2	2990.442	2990.4416	0.16
6_1	5_1			
6_0	5_0			

(c) Assignment of Band C

Standard Dev = 0.0005 cm^{-1}

J' K_c'	J'' K_c''	Calc. ν	Experimental ν	I
0_0	1_0	2986.3451	2986.3451	0.03
1_0	2_0	2985.6308	2985.6304	0.06
1_0	0_0	2987.7656	2987.7656	0.05
1_1	2_1	2985.6295	2985.6291	0.09
1_1	1_1	2987.0528	2987.0522	0.09
2_0	3_0	2984.9136	2984.9144	0.04
2_0	1_0	2988.4718	2988.4718	0.09
2_1	3_1	2984.9124	2984.9130	0.08
2_1	2_1	2987.0473	2987.0468	0.03
2_1	1_1	2988.4705	2988.4705	0.12
2_2	3_2	2984.9088	2984.9088	0.08
2_2	2_2	2987.0436	2987.0431	0.19
3_0	4_0	2984.1937	2984.1948	0.03
3_0	2_0	2987.1751	2989.1748	0.07
3_1	4_1	2984.1925	2984.1936	0.05
3_1	2_1	2989.1739	2989.1736	0.13
3_2	4_2	2984.1889	2984.1930	0.06
3_2	3_2	2987.0354	2987.0354	0.06
3_2	2_2	2989.1703	2989.1699	0.12
3_3	4_3	2984.1828	2984.1838	0.04
3_3	3_3	2987.0293	2987.0288	0.13
4_0	5_0	2983.4711	2983.4709	0.02
4_0	3_0	2989.8757	2989.8754	0.05
4_1	5_1	2983.4699	2983.4699	0.04
4_1	4_1	2987.0280	2987.0288	0.13
4_1	3_1	2989.8745	2989.8742	0.07
4_2	5_2	2983.4662	2983.4663	0.04
4_2	4_2	2987.0244	2987.0247	0.02
4_2	3_2	2989.8709	2989.8705	0.06
4_3	5_3	2983.4601	2983.4599	0.03
4_3	4_3	2987.0183	2987.0184	0.04
4_3	3_3	2989.8648	2989.8645	0.06
4_4	5_4	2983.4516	2983.4511	0.02
4_4	4_4	2987.0098	2987.0097	0.10
5_0	6_0	2982.7457	2982.7447	0.09
5_0	4_0	2990.5736	2990.5734	0.02
5_1	6_1	2982.7445	2982.7437	0.02
5_1	5_1	2987.0145	2987.0151	0.01
5_1	4_1	2990.5724	2990.5723	0.04
5_2	6_2	2982.7408	2982.7402	0.01
5_2	5_2	2987.0106	2987.0114	0.02
5_2	4_2	2990.5687	2990.5689	0.03
5_3	6_3	2982.7348	2982.7340	0.02
5_3	4_3	2990.5627	2990.5626	0.04
5_4	6_4	2982.7262	2982.7260	0.02
5_4	4_4	2990.5542	2990.5546	0.03
5_5	6_5	2982.7153	2982.7150	0.01
5_5	5_5	2986.9851	2986.9857	0.07

(d) Assignment of Band D

Standard Dev = 0.0007 cm^{-1}

J' K_c'	J" K_c"	Calc. ν	Experimental ν	I
0_0	1_0	2986.3997	2986.3988	0.01
1_1	2_1	2985.6838	2985.6834	0.05
1_0	2_0	2985.6857	2985.6853	0.04
1_1	1_1	2987.1069	2987.1066	0.05
1_0	0_0	2987.8203	2987.8204	0.03
2_2	3_2	2984.9619	2984.9621	0.02
2_1	3_1	2984.9673	2984.9674	0.03
2_0	3_0	2984.9692	2984.9691	0.01
2_2	2_2	2987.0965	2987.0960	0.07
2_1	2_1	2987.1020	2987.1017	0.02
2_1	1_1	2988.5251	2988.5253	0.05
2_0	1_0	2988.5270	2988.5271	0.04
3_3	4_3	2984.2338	2984.2344	0.01
3_2	4_2	2984.2429	2984.2441	0.03
3_1	4_1	2984.2484	2984.2494	0.03
3_0	4_0	2984.2505	2984.2512	0.02
3_3	3_3	2987.0780	2987.0795	0.07
3_2	3_2	2987.0891	2987.0888	0.02
3_1	3_1	2987.0946	2987.0960	0.07
3_2	2_2	2989.2238	2989.2240	0.04
3_1	2_1	2989.2293	2989.2288	0.06
3_0	2_0	2989.2311	2989.2305	0.04
4_4	5_4	2983.4995	2983.5000	0.02
4_3	5_3	2983.5123	2983.5117	0.01
4_2	5_2	2983.5215	2983.5220	0.02
4_1	5_1	2983.5269	2983.5270	0.02
4_0	5_0	2983.5288	2983.5289	0.01
4_4	4_4	2987.0573	2987.0578	0.05
4_3	4_3	2987.0701	2987.0696	0.02
4_2	4_2	2987.0793	2987.0795	0.07
4_3	3_3	2989.9164	2989.9145	0.04
4_2	3_2	2989.9255	2989.9261	0.03
4_1	3_1	2989.9310	2989.9312	0.03
4_0	3_0	2989.9328	2989.9329	0.02
5_2	6_2	2982.7976	2982.7975	0.01
5_1	6_1	2982.8031	2982.8019	0.01
5_0	6_0	2982.8049	2982.8027	0.01
5_2	4_2	2990.6247	2990.6260	0.02
5_1	4_1	2990.6302	2990.6306	0.02
5_0	4_0	2990.6321	2990.6323	0.01

Transitions	Calculation (cm^{-1})	Observed (cm^{-1})	Residual (cm^{-1})
$0^- \rightarrow 1^-$	198.75	198.6	0.15
$1^- \rightarrow 2^-$	175.71	176.1	0.60
$2^+ \rightarrow 3^+$	117.87	117.4	0.47
$2^- \rightarrow 3^-$	175.36	174.8	-0.44
$3^+ \rightarrow 4^+$	176.51	174.9	1.61
$3^- \rightarrow 4^-$	205.08	204.1	0.98
$4^- \rightarrow 5^-$	221.23	220.1	1.13
$4^+ \rightarrow 5^+$	236.99	236.0	0.99
$5^+ \rightarrow 6^+$	250.95	250.1	0.85
$5^- \rightarrow 6^-$	263.82	263.0	0.83